Supplementary information on
Symmetric quantum dots as efficient sources of highly entangled photons: *violation of Bell's inequality without spectral and temporal filtering*

Takashi Kuroda,[1,2,*] Takaaki Mano,[1] Neul Ha,[1,2] Hideaki Nakajima,[1,3]
Hidekazu Kumano,[3] Bernhard Urbaszek,[4] Masafumi Jo,[1] Marco Abbarachi,[1]
Yoshiki Sakuma,[1] Kazuaki Sakoda,[1] Ikuo Suemune,[3] Xavier Marie,[4] and Thierry Amand[4]

[1] *National Institute for Materials Science, 1 Namiki, Tsukuba 305-0044, Japan*
[2] *Graduate School of Engineering, Kyushu University, Japan*
[3] *Research Institute for Electronic Science, Hokkaido University, Sapporo 001-0021, Japan*
[4] *Université de Toulouse, INSA-CNRS-UPS, LPCNO, 135 avenue de Rangueil, 31077 Toulouse, France*

(Dated: July 5, 2013)

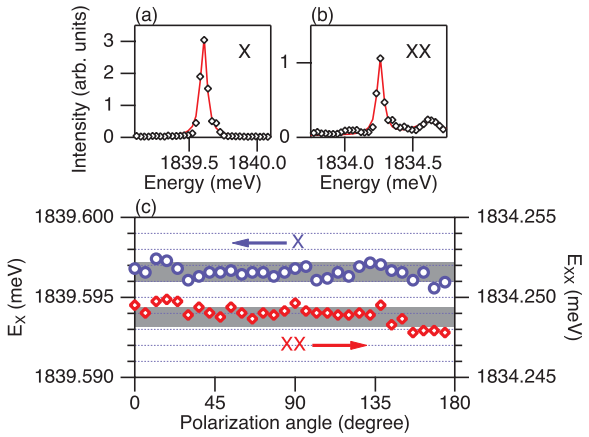

Supplementary Figure 1. (a) The X line PL spectrum detected by a charge-coupled devise detector (black diamonds) and its Lorentzian fit (red line). (b) The XX line PL spectrum. (c) Peak energies of X ($E_{\rm X}$, blue circles) and XX ($E_{\rm XX}$, red diamonds) as a function of the angle of linearly-polarized projection. The shaded area shows the radiatively-limited spectral width (1.2 μeV in FWHM). They are studied in the same dot as that used in the correlation measurement.

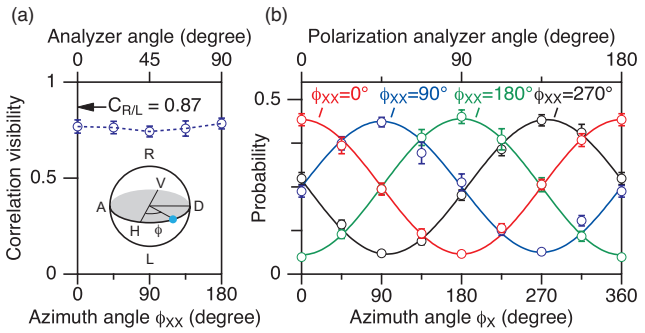

Supplementary Figure 2. Photon correlations using linear polarization bases. (a) The correlation visibility (C) of linear polarizations for different polarization angles. The angle used in these plots is defined as the azimuth angle (ϕ) of a polarization state that moves in the equator of the Poincaré sphere ($\phi = 0$ for H and $\phi = 90^\circ$ for D). Note that ϕ is double the angle of a polarization analyzer. There is no significant dependence of C on the polarization angle within error. The higher C value for circular bases, indicated by an arrow, is related to exciton depolarization due to nuclear fluctuations. See, Supplementary Discussion for detail. (b) Normalized coincidence counts as a function of the X polarization angle ($\phi_{\rm X}$) for four different values of the XX polarization ($\phi_{\rm XX}$). The error bars include only Poissonian noise. The sinusoidal fits are also shown by lines. The S parameter is estimated to be 2.03 ± 0.08 for these polarization sets. The S value is lower than that estimated in the main text because of the use of different measurement bases and the fact that $C_{R/L} > C_{H/V} \approx C_{D/A}$.

Supplementary Discussion

Source of entanglement degradation. The degree of quantum interference is suppressed by the presence of incoherent light. If its spectrum coincides with the XX and X lines, unwanted photons would reach the detectors and mask the interference. However, we expect the photon noise to be negligible because of the fact that the correlation visibility is independent of the bandpass of the spectral filters, which are varied from 60 to 200 μeV. Another potential source of entanglement degradation, which has recently been pointed out, is recapture [1, 2]. In this process, the intermediate X state is re-excited to the XX state before recombination, along with the capture of hot carriers or the reabsorption of pump light. Recapture leads to the emission of more than two photons per excitation cycle and these photons act as noise. However, we do not expect recapture to play a major role in the present case. The experiments were carried out at sufficiently low excitation power, and we observe an asymmetric coincidence profile, which confirms that the photon pairs come from a clean cascade. Here we discuss the effect of exciton depolarization on quantum interference, which has thus far been overlooked.

Exciton depolarization is associated with asymmetric environmental motion, which includes the charge and nuclear fluctuations in the vicinity of a dot. Any asymmetric perturbation can lift the exciton degeneracy. Note that, if the energy shift is constant, the time-resolved emissions show temporal oscillations in the polarization degree due to the superposition of the split eigenstates. If the energy shift changes randomly, the polarization degree becomes quenched through ensemble (time) averaging. The correlation visibility is thus estimated as $\Gamma_1/(\Gamma_1+\Delta)$, where Γ_1 is the recombination rate, and Δ is the standard deviation of the fluctuating exciton splits. The effect of a slowly varying environment is probably the last remaining source which limits the degree of quantum interference in the solid-state photon source.

We observe that the correlation visibility is higher for a circular polarization basis than linear polarization bases, i.e., $C_{R/L} > C_{H/V} = C_{D/A}$. The same signature has been observed previously [1, 2]. We interpret this orientation dependent depolarization in terms of the fluctuating electric fields (with localized charges) and magnetic fields (with nuclei). Since a vertical electric field does not break the rotational symmetry, only an in-plane electric field gives rise to the degeneracy lift of the exciton state. A frozen in-plane field along x splits the exciton state into linearly polarized states, which lead to the observation of $C_{x/y} > C_{x+45^\circ/y+45^\circ} = C_{R/L}$. If the electric field fluctuates randomly in all directions, the polarization degree becomes isotropic so that $C_{H/V} = C_{D/A} = C_{R/L}$.

In a GaAs quantum dot the carrier spins are interacting with the nuclear spins of the atoms that form the dot [3]. In the absence of optical pumping, the mean value of the nuclear spin polarization (represented by an effective magnetic field B_n called Overhauser field) is zero, but the carrier spins are subject to the field fluctuations δB_n, which is in the tens of mT range. Since the nuclear spin configuration changes randomly on a ms time-scale, we average over all possible orientations of δB_n in the present experiments.

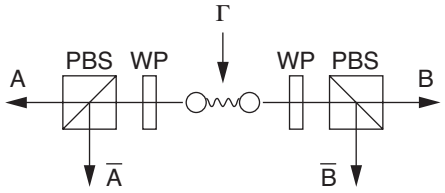

Supplementary Figure 3. Photon correlation setup. Photon pairs are generated with a probability of Γ. Each photon is projected to a specific measurement base, using an appropriate wave plate (WP) followed by a polarization beam splitter (PBS).

The effect of δB_n on the bright X states depends on the orientation [4]. (i) A transverse (in-plane) component ($\delta B_n^{\mathrm{T}} \perp [111]$) induces electron spin precession and couples the bright X state $|+1\rangle$ ($|-1\rangle$) to the dark X state $|+2\rangle$ ($|-2\rangle$). The bright states and the dark states are separated by the isotropic electron hole exchange splitting $\delta_0 \approx 350$ μeV in our dot sample [5]. The coupling strength and the associated energy renormalization scale as the ratio $|\delta_n|/\delta_0$, where $|\delta_n| = g_e\mu_B|\delta B_n|$ with $g_e = 0.5$ for our dot [6] and μ_B is the Bohr magneton ($\mu_B = 57.9$ μeV/T). In our system a typical value of $|\delta B_n| = 10$ mT corresponds to $|\delta_n| = 0.25$ μeV and hence $|\delta_n| \ll \delta_0$. As a consequence, the effect of the in-plane component of δB_n on the X energy and polarization is negligible. (ii) A longitudinal component ($\delta B_n^{\mathrm{L}} \parallel [111]$) has two effects. First, it increases the FSS from the initial value of δ_1 to $\sqrt{\delta_1^2 + (g_e\mu_B\delta B_n)^2}$. If δ_1 is negligible, the energy shift is approximated as $|\delta_n|$. Second, the X eigenstates become more circular and as a result $C_{R/L} > C_{H/V} = C_{D/A}$. Using $|\delta_n| = 0.25$ μeV one would expect to find $C_{R/L} - C_{H/V} = |\delta_n|/\Gamma_1 = 0.1$, which is in excellent agreement with the experimental results. Thus, the nuclear field fluctuations introduce an additional anisotropy that needs to be controlled to optimize the degree of entanglement.

Supplementary Method

Normalization procedure used in the correlation analysis. A typical setup for measuring the polarization correlations is shown in Supplementary Fig. 3. Photon pairs, which are generated with a rate of Γ, are divided into two photons, either of which is projected on a polarization base of A, and the other is projected on a polarization base of B. Polarization beam splitters transmit the projected photons, and reflect the orthogonal complements, $\bar{A}$ and $\bar{B}$. The number of coincidence per unit

time (N_{AB}) is expressed by,

$$N_{AB} = \Pr(A \cap B)\Gamma\, \eta_A \eta_B, \tag{1}$$

where $\Pr(A \cap B)$ is the joint probability that one photon is projected along A, and the other is projected along B. η_A (η_B) is the counting efficiency for A (B) projected photons. The final purpose of this measurement is the estimation of $\Pr(A \cap B)$. Equation 1 contains an unknown factor of $\Gamma\eta_A\eta_B$, which can be determined separately in principle. However, for a dot-based source, this factor fluctuates in time (due to the small vibration of the micro-objective setup), and its precise determination is practically impossible. Here we describe that adequate two-step normalizations ideally remove the effect of the fluctuations.

The first normalization is based on the number of accidental coincidence. It is counted simultaneously with "true" coincidence, and appears as side peaks in the coincidence histogram. Hereafter, we assume that XX photons are projected on A, and X photons are projected on B. The number of accidental coincidence is given by,

$$N_{AB}^{\rm side} = p_A \Gamma_{\rm XX}\, \eta_A \times p_B \Gamma_{\rm X}\, \eta_B, \tag{2}$$

where p_A is the probability of finding A polarized XX photons, and p_B is that of finding B polarized X photons. We are able to determine p_A and p_B by performing a standard photoluminescence measurement. $\Gamma_{\rm XX}$ ($\Gamma_{\rm X}$) is the probability that XX (X) occupies the dot. Note that $\Gamma = \Gamma_{\rm XX} \leq \Gamma_{\rm X}$ for the dot-based sources [7]. We define a normalized coincidence count as,

$$n_{AB} \equiv \frac{N_{AB}}{N_{AB}^{\rm side}} = \frac{1}{\Gamma_{\rm X}\, p_A p_B} \Pr(A \cap B). \tag{3}$$

Note that the factor $\eta_A\eta_B$ in Eq. 1 disappears in Eq. 3. Thus, n_{AB} is not affected by the fluctuation of collection efficiencies.

Equation 3 still contains a parameter of Γ_X that fluctuates with time. The relevant effect will be removed by the second normalization, which uses the number of coincidence with the orthogonal complement. Here we simultaneously count $\bar{B}$ polarized X photons and integrate $n_{A\bar{B}}$ along with n_{AB}. We define $\Pr(B|A)$ as the conditional probability that X photons are projected along B, given that XX photons are projected along A, so that

$$\Pr(B|A) = \frac{\Pr(A \cap B)}{p_A}, \tag{4}$$

According to the definition of projection measurements, we have

$$\Pr(B|A) + \Pr(\bar{B}|A) = 1. \tag{5}$$

The above relation allows us to normalize n_{AB} and $n_{A\bar{B}}$, and finally obtain

$$\Pr(B|A) = \frac{p_B\, n_{AB}}{p_B n_{AB} + p_{\bar{B}} n_{A\bar{B}}}, \tag{6}$$

$$\Pr(\bar{B}|A) = \frac{p_{\bar{B}}\, n_{A\bar{B}}}{p_B n_{AB} + p_{\bar{B}} n_{A\bar{B}}}, \tag{7}$$

and thus

$$\Pr(A \cap B) = \frac{p_A p_B\, n_{AB}}{p_B n_{AB} + p_{\bar{B}} n_{A\bar{B}}}, \tag{8}$$

$$\Pr(A \cap \bar{B}) = \frac{p_A p_{\bar{B}}\, n_{A\bar{B}}}{p_B n_{AB} + p_{\bar{B}} n_{A\bar{B}}}. \tag{9}$$

Note that the above forms are free from any fluctuating factor.

To test the CHSH inequality, we measure the degree of correlation for A projected photons and B projected photons, i.e.,

$$C_{A/B} = \Pr(A \cap B) - \Pr(A \cap \bar{B}) - \Pr(\bar{A} \cap B) + \Pr(\bar{A} \cap \bar{B}). \tag{10}$$

Then, the CHSH equality is given by

$$S = C_{A/B} + C_{A'/B} - C_{A/B'} + C_{A'/B'} < 2. \tag{11}$$

In the present experiment, we confirmed that both XX and X emissions are unpolarized within an error of 5 %. If we assume a perfectly unpolarized source so that $p_A = p_{\bar{A}} = p_B = p_{\bar{B}} = 1/2$, the above forms become,

$$\Pr(A \cap B) = \frac{1}{2}\frac{n_{AB}}{n_{AB} + n_{A\bar{B}}}, \tag{12}$$

$$\Pr(A \cap \bar{B}) = \frac{1}{2}\frac{n_{A\bar{B}}}{n_{AB} + n_{A\bar{B}}}. \tag{13}$$

They are used to plot Fig. 3(a) in the main text and Supplementary Fig. 1(b).

* kuroda.takashi@nims.go.jp

[1] R. J. Young, R. M. Stevenson, A. J. Hudson, C. A. Nicoll, D. A. Ritchie, and A. J. Shields, Phys. Rev. Lett. **102**, 030406 (2009).

[2] A. Dousse, J. Suffczyǹski, A. Beveratos, O. Krebs, A. Lemaître, I. Sagnes, J. Bloch, P. Voisin, and P. Senellart, Nature **466**, 217 (2010).

[3] T. Belhadj, T. Kuroda, C.-M. Simon, T. Amand, T. Mano, K. Sakoda, N. Koguchi, X. Marie, and B. Urbaszek, Phys. Rev. B **78**, 205325 (2008).

[4] R. M. Stevenson, C. L. Salter, A. Boyer de la Giroday, I. A. Farrer, C. A. Nicoll, D. A. Ritchie, and A. J. Shields, "Coherent entangled light generated by quantum dots in the presence of nuclear magnetic fields," arXiv:1103.2969 (2011).

[5] G. Sallen, B. Urbaszek, M. M. Glazov, E. L. Ivchenko, T. Kuroda, T. Mano, S. Kunz, M. Abbarchi, K. Sakoda, D. Lagarde, A. Balocchi, X. Marie, and T. Amand, Phys. Rev. Lett. **107**, 166604 (2011).

[6] M. V. Durnev, M. M. Glazov, E. L. Ivchenko, M. Jo, T. Mano, T. Kuroda, K. Sakoda, S. Kunz, G. Sallen, L. Bouet, X. Marie, D. Lagarde, T. Amand, and B. Urbaszek, Phys. Rev. B **87**, 085315 (2013).

[7] T. Kuroda, T. Belhadj, M. Abbarchi, C. Mastrandrea, M. Gurioli, T. Mano, N. Ikeda, Y. Sugimoto, K. Asakawa, N. Koguchi, K. Sakoda, B. Urbaszek, T. Amand, and X. Marie, Phys. Rev. B **79**, 035330 (2009).